Role of Arginine-82 in Fast Proton Release during the Bacteriorhodopsin Photocycle: A Time-Resolved FT-IR Study of Purple Membranes Containing ^{15}N-Labeled Arginine†

Yaowu Xiao,‡ M. Shane Hutson,‡,§ Marina Belenky,|| Judith Herzfeld,|| and Mark S. Braiman*,‡

Department of Chemistry, Syracuse University, Syracuse, New York 13244-4100, and Department of Chemistry, Brandeis University, Waltham, Massachusetts 02454-9110

Received April 16, 2004; Revised Manuscript Received June 18, 2004

ABSTRACT: Arginine-82 has long been recognized as an important residue in bacteriorhodopsin (bR), because its mutation usually results in loss of fast H^+ release, an important step in the normal light-induced H^+ transport mechanism. To help to clarify the structural changes in Arg-82 associated with the H^+-release step, we have measured time-resolved FT-IR difference spectra of wild-type bR containing either natural-abundance isotopes (^{14}N-Arg-bR) or all seven arginines selectively and uniformly labeled with ^{15}N at the two η-nitrogens (^{15}N-Arg-bR). Comparison of the spectra from the two isotopic variants shows that a 1556 cm^{-1} vibrational difference band due to the M photocycle intermediate of ^{14}N-Arg-bR loses substantial intensity in ^{15}N-Arg-bR. However, this isotope-sensitive arginine vibrational difference band is only observed at pH 7 and not at pH 4 where fast H^+ release is blocked. These observations support the earlier conclusion, based on site-directed mutagenesis and chemical labeling, that a strong C−N stretch vibration of Arg-82 can be assigned to a highly perturbed frequency near 1555 cm^{-1} in the M state of wild-type bR [Hutson et al. (2000) *Biochemistry 39*, 13189−13200]. Furthermore, alkylguanidine model compound spectra indicate that the unusually low arginine C−N stretch frequency in the M state is consistent with a nearly stoichiometric light-induced deprotonation of an arginine side chain within bR, presumably arginine-82.

Bacteriorhodopsin (bR),[1] a retinal protein found in the archaeal genus *Halobacterium*, acts as a light-driven H^+ pump (*1*−*4*). Upon absorption of a photon, the first step in the bR photocycle is the isomerization of the all-*trans*-retinal to 13-*cis*. This process is extremely fast, giving rise to the primary photoproduct K state of bR in <5 ps (*5*, *6*). From the K state, bR relaxes through a series of photointermediates, L through O, involving backbone conformational changes and H^+ movements. The net result of the sequence of H^+-transfer reactions is the transport of a H^+ from the cytoplasmic to the extracellular side of the membrane.

Figure 1 describes the key H^+ movements in the bR photocycle, with a curved arrow to indicate the location of the bond around which retinal twists in the K formation. The first of the H^+ transfers is from the protonated retinal Schiff base to the anionic Asp-85. This occurs during the L → M conversion (*8*), which has a time constant of ∼50 μs (*9*). Nearly coincident, at physiological pH, is H^+ release to the extracellular surface (*10*−*12*). Since Asp-85 remains protonated at least throughout the lifetime of M (∼5 ms), the H^+ released into the extracellular medium on a time scale of ∼50 μs cannot originate directly from the protonated Schiff base. It was therefore proposed that this fast extracellular H^+ release is mediated by a different H^+ donor group (*8*, *13*). This group serves as the source of the fast-released H^+ under normal conditions and is termed the proton release group (PRG).

Direct evidence for the existence and function of the PRG could be inferred from time-resolved experiments in which the released protons were monitored by pH indicator dyes in the bulk aqueous medium (*14*). Such experiments, in combination with site-directed mutations, have led to suggestions about the identity of the PRG. The matter has nevertheless remained murky due to results implicating a number of residues, as well as water molecules. Possible PRG candidates include Glu-204 (*15*−*18*), Glu-194 (*19*), Arg-82 (*20*−*22*), and H_2O (*23*, *24*), all encompassed by the circle in Figure 1 and all implicated in what has been termed the proton release complex (*20*). Definitive identification of the PRG should theoretically be possible through FT-IR difference spectroscopy and/or solid-state NMR spectroscopy.

In the past, time-resolved FT-IR difference spectroscopy has identified protonation changes of such important residues as Asp-85 and Asp-96 in different photocycle intermediates (*25*−*27*). Similar FT-IR experiments on wild-type bR can be expected to help to clear up the ambiguities about the

† This work was supported by the Keck Center for Molecular Electronics at Syracuse University and by NIH Grant EB001035 to J.H.

* Corresponding author: telephone, 315-443-4691; fax, 315-443-4070; e-mail, mbraiman@syr.edu.

‡ Syracuse University.

§ Current address: Physics Department, Vanderbilt University, 1807 Station B, Nashville, TN 37235.

|| Brandeis University.

[1] Abbreviations: bR, bacteriorhodopsin; PRG, proton release group; DTEG, *S*-decylthioethylguanidinium.

10.1021/bi049238g CCC: $27.50
Published on Web 09/18/2004

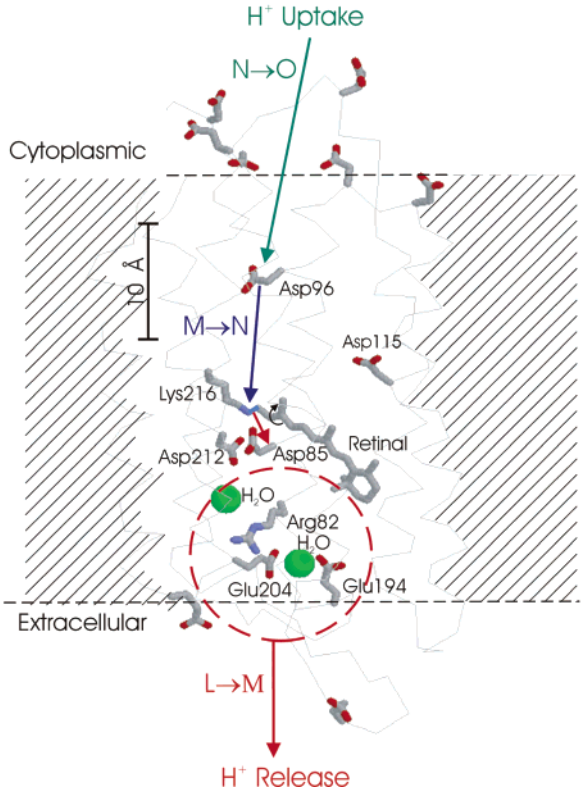

FIGURE 1: Structure of the M state of bacteriorhodopsin, based on published atomic coordinates (*7*), showing the location of key ionizable residues and the paths of H^+ transfers during the photocycle (red, L → M; blue, M → N; and green, N → O) as deduced from time-resolved spectroscopic measurements.

PRG remaining from the experiments on mutants. First, the transient deprotonation of the PRG in the M state is expected to result in vibrational bands in the bR → M difference spectrum which should be sensitive to isotope labeling of the PRG. Second, the PRG bands in the difference spectrum should have a characteristic pH dependence. At pH values below 5.8 H^+ release is delayed, so that the temporal sequence of H^+ release and uptake is reversed (*28*, *29*). Therefore, comparison of wild-type bR → M difference spectra at pH values below and above 5.8 should lead to identification of IR bands arising from the PRG.

In the current work, time-resolved FT-IR difference spectra have been measured for bR intermediates in the wild-type protein, containing either natural-abundance isotopes (^{14}N-Arg-bR) or ^{15}N selectively and uniformly incorporated into the two η positions of each of the arginine residues (^{15}N-Arg-bR). Comparison of the spectra from the two proteins shows that the 1556 cm^{-1} band due to M in ^{14}N-Arg-bR reproducibly loses substantial intensity in ^{15}N-Arg-bR. Therefore, a strong C−N stretch vibration of Arg-82 can indeed be assigned to a highly perturbed frequency near 1556 cm^{-1} in the M state of wild-type bR. This surprisingly low C−N stretch vibrational frequency is also observed in arginine model compounds containing a deprotonated guanidine group, providing some support for the hypothesis that Arg-82 itself functions as the PRG in bR.

MATERIALS AND METHODS

Sample Preparation. All samples were of wild-type bR in its native purple membrane. The natural-abundance (^{14}N-Arg-bR) sample was isolated from the S9 strain of *Halobacterium salinarum*. Preparation of the isotope-labeled sample, ^{15}N-Arg-bR, was described previously (*30*). The same sample has been used to observe the asymmetric environment of Arg-82 in the M state of bR by solid-state NMR (*30*). Co-incorporation of trace [ξ-^{14}C]Arg, as determined by extraction and amino acid analysis, indicated that the guanidyl group was 90% labeled, with no scrambling to other amino acid residues, lipid, or chromophore (*30*).

Samples of protein for FT-IR measurement were prepared as described previously (*21*). A purple membrane suspension was washed twice in an appropriate buffer solution (25 mM sodium phosphate at pH 7 or 25 mM sodium acetate at pH 4) and pelleted in a microcentrifuge. The pellet was then sealed between two CaF_2 windows using vacuum grease around the perimeter. The sample thickness was typically 6−10 μm, and the water content of the samples ranged from ∼50% to 80% (w/w) and is specifically indicated in individual figure legends. It was determined by comparing the ratio of the 1650 and 1550 cm^{-1} bands in the static IR absorbance spectrum to a previously published set of reference spectra (*31*).

Time-Resolved FT-IR Measurements. A Nicolet Magna-IR 860 spectrometer operated in step-scan mode with a 20 MHz bandwidth photovoltaic HgCdTe detector/preamplifier operating with DC-coupled output. A pulsed, frequency-doubled Nd^+-YAG laser (532 nm, 10 mJ cm^{-2} per flash) was used to initiate the photocycle repeatedly. Spectra were recorded with 8 cm^{-1} resolution at 20 °C, with an interval between laser flashes of 0.3 s, or with 4 cm^{-1} resolution at 0 °C, with an interval of 1.5 s. Under both temperature conditions, an external amplifier with a gain of 25 was applied to the transient signals to maximally utilize the ±10 V range of the internal digitizer board. The step-scan software was set so that the interferometer's retardation steps were equal to 4 times the HeNe laser wavelength, i.e., ∼2.5 μm. This widely spaced sampling of the interferogram was possible, without introducing aliasing artifacts, because the optical bandwidth of the measurement was reduced by placing a long-pass optical filter with a cutoff wavelength of 5 μm in the IR beam between the sample and detector. The same optical filter also blocked scattered light from the Nd^+-YAG laser.

Synthesis of Model Compounds. Thioethylguanidinium bromide (TEG-Br) was synthesized from thiourea and 2-bromoaminoethane (Aldrich) by a previously published method (*32*). Through the use of [^{15}N]thiourea as a starting material (Cambridge Isotope Laboratories), isotope labels were incorporated at the terminal nitrogens, N_η, of the TEG-Br guanidino group. *S*-Decylthioethylguanidinium (DTEG) bromide was prepared from the reaction between TEG-Br and 1-bromodecane (in C_2H_5OH, under reflux). The presence of the long decyl chain makes the guanidino salt sufficiently soluble in $CHCl_3$ to measure readily interpretable FT-IR spectra.

RESULTS

bR → M Difference Spectra at 20 °C and pH 7. Figure 2a shows the time-resolved FT-IR photoproduct difference spectra for ^{14}N-Arg-bR and ^{15}N-Arg-bR at 20 °C and pH 7, averaged over the period 50−500 μs. (The region between

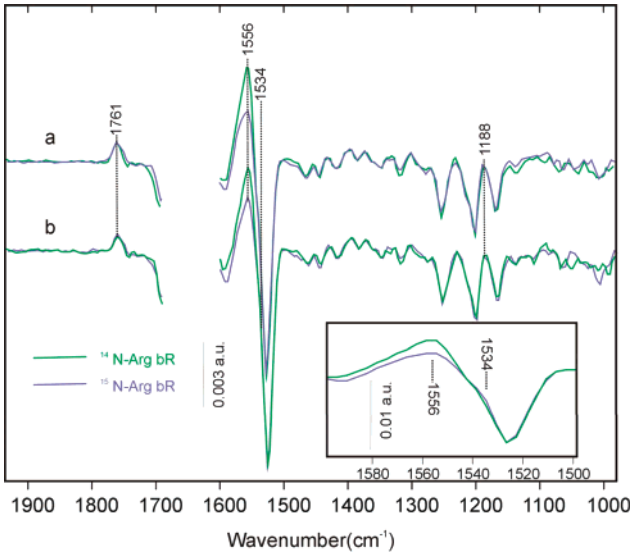

FIGURE 2: Average time-resolved FT-IR spectra of ^{14}N-Arg-bR (green) and ^{15}N-Arg-bR (purple) collected from 50 to 500 μs at room temperature. Spectra were all normalized to the negative band at 1527 cm^{-1}. The 1600−1700 cm^{-1} region was blanked because of its significantly worse signal/noise ratio. The upper and lower pairs of traces were measured with different bR samples to show the reproducibility of the isotope-induced changes. Water contents in the four different samples were all within 5% of each other and in the range of ~75% (w/w) overall. Inset: Expansion of the 1500−1580 cm^{-1} region showing more clearly the positive IR intensity downshifted from 1556 cm^{-1} (for ^{14}N-Arg-bR) to 1534 cm^{-1} (for ^{15}N-Arg-bR). The spectra are pairwise averages of those in (a) and (b).

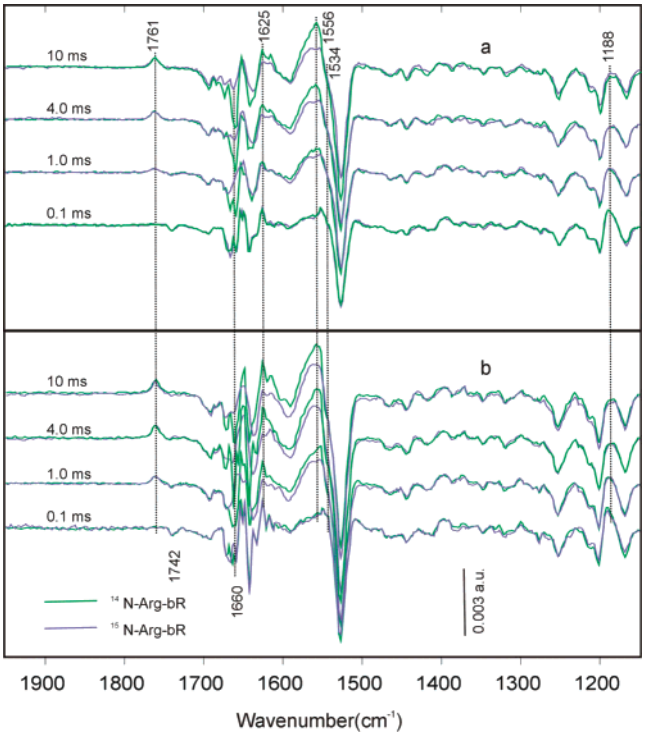

FIGURE 3: Time-resolved FT-IR spectra of ^{14}N-Arg-bR (green) and ^{15}N-Arg-bR (purple) at 4 cm^{-1} resolution collected at 0 °C. The spectra in each panel are stacked in ascending order from 0.1 to 10 ms after the flash. Results from two different pairs of bR samples, shown in panels a and b, demonstrate the degree of reproducibility. Water content in (a) was 50% for ^{14}N-Arg-bR and 57% for ^{15}N-Arg-bR. For (b), the respective water contents were 64% and 62%.

1600 and 1700 cm^{-1} was blanked in this figure because of the effect on signal/noise of the high background absorbance from the H−O−H and amide I vibrations centered near 1650 cm^{-1}.) Several features of the spectra show that the dominant photointermediate present over this time range is M. These features include a positive band due to the COOH stretch of Asp-85 at 1761 cm^{-1} (with no evidence of a partial shift to 1754 cm^{-1} as occurs during the M → N transition) and a characteristic 13-*cis*-retinylidene C−C stretch band with a maximum differential intensity at 1188 cm^{-1} that remains slightly below the zero absorbance baseline.

Although the two isotopic variants' spectra in Figure 2a correspond closely in general, a substantial difference exists in absorbance intensities around 1556 cm^{-1}. The 1556 cm^{-1} positive difference band in the ^{14}N-Arg-bR spectra clearly decreases in the ^{15}N-Arg-bR spectra. This is presumably the result of the frequency downshift of a vibration involving significant nitrogen motion. In fact, the downshifted frequency in the ^{15}N-Arg-bR spectrum can be assigned at ~1534 cm^{-1}, in a region of the difference spectrum with too large a slope to see the change easily. This downshifted band can be clearly visualized, however, by calculation of a double-difference spectrum (see below). The reproducibility of the observation of the isotope-induced downshift in the 1556 cm^{-1} band is demonstrated by the spectra of distinct bR samples in Figure 2b.

BR → M Difference Spectra Collected at 0 °C and pH 7. To observe the time-dependent isotope effects on the 1556 cm^{-1} band more clearly, further time-resolved measurements were carried out at 0 °C. The longer lifetime of the M intermediate at this temperature allowed more difference spectra to be averaged together, which resulted in better signal/noise ratio. A series of time-resolved FT-IR difference spectra for ^{14}N-Arg-bR and ^{15}N-Arg-bR, covering a time range of 0.1−10 ms after photolysis, are stacked in Figure 3a. Figure 3b was recorded under the same conditions, but with different ^{14}N-Arg-bR and ^{15}N-Arg-bR samples, to show the reproducibility of the band differences around 1556 and 1660 cm^{-1}.

In Figure 3a, the earliest (0.1 ms) spectra are similar for both proteins, showing no obvious isotope labeling effects. They show a clear negative band at 1742 cm^{-1}, associated with a change in protonation state and/or H-bonding environment of the Asp-96 COOH group known to occur in the L state. This negative 1742 cm^{-1} band disappears in later spectra, accompanied by a rise of the positive 1761 cm^{-1} band indicating the L → M conversion. Spectra measured at later time points, where M is predominant, reproduce the isotope-induced downshift observed near 1556 cm^{-1} at room temperature (Figure 2). More specifically, the isotope-induced intensity difference of the band at 1556 cm^{-1} grows on the time scale of M formation. The magnitude of this intensity difference is comparable to that of the positive 1761 cm^{-1} band. Once again, the downshifted frequency for ^{15}N-Arg-bR is near 1534 cm^{-1}, as calculated from double-difference spectra (see next subsection and Figure 4).

Another isotope-induced difference is that the bR → M difference spectrum for ^{15}N-Arg-bR shows a decrease in amplitude for the negative band at 1660 cm^{-1}, relative to ^{14}N-Arg-bR, as well as a decrease in amplitude for a positive band near 1625 cm^{-1}.

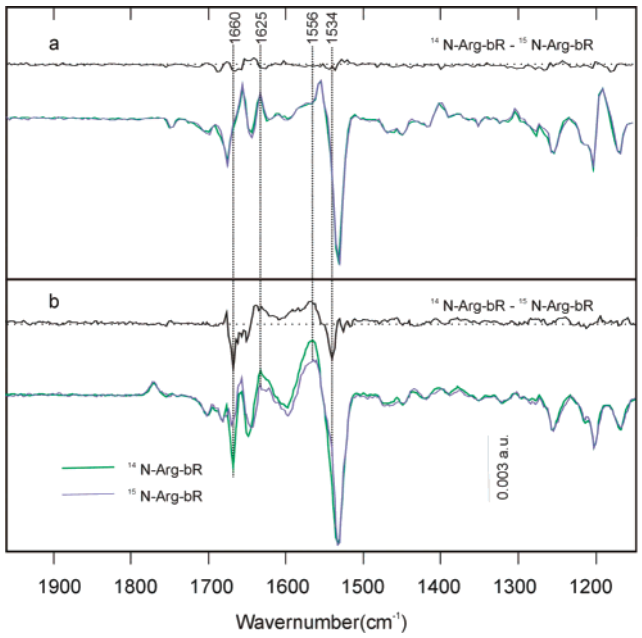

FIGURE 4: Time-resolved difference spectra and isotope substitution double-difference spectra for the L and M states. (a) Below: The bR → L spectra for ^{14}N-Arg-bR (green) and ^{15}N-Arg-bR (purple), each obtained as the initial difference spectrum (i.e., the spectrum obtained by extrapolating back to time zero) from a global multiexponential fit of the bR photocycle over the time range 0.06−10 ms at 0 °C. Above: Double-difference FT-IR spectrum corresponding to (^{14}N-Arg-bR → L) minus (^{15}N-Arg-bR → L). (b) Below: Calculated bR → M difference spectra for ^{14}N-Arg-bR (green) and ^{15}N-Arg-bR (purple), each obtained from the faster decaying amplitude spectrum (L → M) minus the corresponding initial spectrum (bR → L). Above: Double-difference FT-IR spectrum corresponding to (^{14}N-Arg-bR → M) minus (^{15}N-Arg-bR → M).

From Figures 2 and 3, isotope labeling strongly supports assignment of a substantial portion of the positive band at ∼1556 cm^{-1} to a C−N$_\eta$ stretch vibration of ^{14}N-Arg-bR in the M state. The isotope labeling is also consistent with the assignment of a negative band at ∼1660 cm^{-1} to the highest frequency C−N$_\eta$ stretch vibration of ^{14}N-Arg-bR in the unphotolyzed bR state.

Kinetic Analysis of FT-IR Difference Spectra Collected at 0 °C and pH 7. One advantage of using the DC-coupled detector output to record time-resolved FT-IR difference spectra is that this eliminates the ∼800 μs instrumental time constant of the AC-coupled digitizer board. This allows recording of time-resolved spectra that are directly suitable for global multiexponential fit. It has been reported (*9*, *33*, *34*) that, in a global fit, at least six exponentials plus a constant difference spectrum are necessary to describe completely the bR photocycle. However, in our experiment at 0 °C, only part of the photocycle is observed due to the limited time range (0.06−10 ms; the first 30 μs slice after photolysis was not included in the fit, because it was heavily affected by the low-pass electronic filter on the detector). Therefore, only two exponentially decaying spectra plus a constant-amplitude spectrum were needed to fit the spectra in Figure 3a using the FITEXP program (*35*, *36*). The fitted time constants for the two transients are 522 ± 64 and 4274 ± 872 μs for ^{14}N-Arg-bR and 503 ± 100 and 4370 ± 940 μs for ^{15}N-Arg-bR, respectively. Because of the truncated description of the photocycle, the spectra obtained by the analysis may be distorted for the last intermediate, but the earlier spectra are not influenced by the limited data acquisition period.

The initial spectrum, shown in Figure 4a, corresponds to a rather pure bR → L difference spectrum. This is indicated from the characteristic negative 1742 cm^{-1} band, due to the protonated Asp-96 group present in the bR state, and the large positive 1188 cm^{-1} band, due to a chromophore vibration of the 13-*cis*-retinylidene protonated Schiff base state present in L. The fitted initial (bR → L) difference spectra for ^{14}N-Arg-bR and ^{15}N-Arg-bR show no significant isotope-induced effects in the region around 1556 and 1660 cm^{-1}. This is more clearly verified by the (^{14}N-Arg-bR → L) minus (^{15}N-Arg-bR → L) double-difference spectrum, as shown at the top of Figure 4a. Here the few small bands observed above the noise level represent the limits of the accuracy of the phase correction of the differential FT-IR signals.

The first time-dependent amplitude spectrum obtained from the FITEXP program has a ∼500 μs decay time, in reasonable agreement with previously published values for the L → M transition near 0 °C (*9*), and is therefore expected to correspond to an L → M difference spectrum. By subtracting the bR → L difference spectrum (corresponding to the initial spectrum from the multiexponential fit), it is possible to obtain the bR → M difference spectrum shown in Figure 4b. After this subtraction, there is no discernible negative band at 1742 cm^{-1}, consistent with previously published bR → M spectra that have led to the conclusion that Asp-96 and Asp-115 do not experience perturbations during this photoreaction (*37*). The calculated bR → M spectra for both isotope variants are shown in Figure 4b (bottom) and are used to calculate the (^{14}N-Arg-bR → M) minus (^{15}N-Arg-bR → M) double-difference spectrum (Figure 4b, top). This double-difference spectrum reveals a very clear pair of double difference bands at 1556 and 1534 cm^{-1}. These result from the downshift of the positive band at 1556 cm^{-1} in the ^{14}N-Arg-bR → M difference spectrum to 1534 cm^{-1} in the ^{15}N-Arg-bR → M spectrum, i.e., at the same positions observed in the higher temperature data in Figures 2 and 3.

bR → M Difference Spectra Collected at 0 °C and pH 4. Figure 5 compares average time-resolved FT-IR difference spectra collected at 0 °C and pH 4 with those obtained at pH 7. At pH 4 as at pH 7, the two isotope variants show similar photocycle kinetics, with M rise times of 624 ± 99 and 570 ± 87 μs for ^{14}N-Arg-bR and ^{15}N-Arg-bR, respectively, i.e., just slightly slower than at pH 7. It is known that there is virtually no buildup of later intermediates (e.g., N or O) at 0 °C and either pH 4 or pH 7 (*9*). Therefore, the spectra in Figure 5, covering the 5−10 ms interval, also represent almost pure bR → M difference spectra. At pH values below 5, bR is known to lose its capacity for fast light-induced H$^+$ release (*29*). Therefore, the bR → M spectrum at pH <5 is expected to show an absence of vibrational bands associated with structural changes in the H$^+$-release group that are present at higher pH.

One previously reported effect of lowering pH on bR → M difference spectra is an upshift of the C=O stretch frequency from Asp-85. It is located at 1760 cm^{-1} at neutral pH and at 1762 cm^{-1} at acidic pH (*38*). This 2 cm^{-1} shift was taken to indicate a slight decrease of the environmental dielectric constant around Asp-85 at lower pH. Our spectra

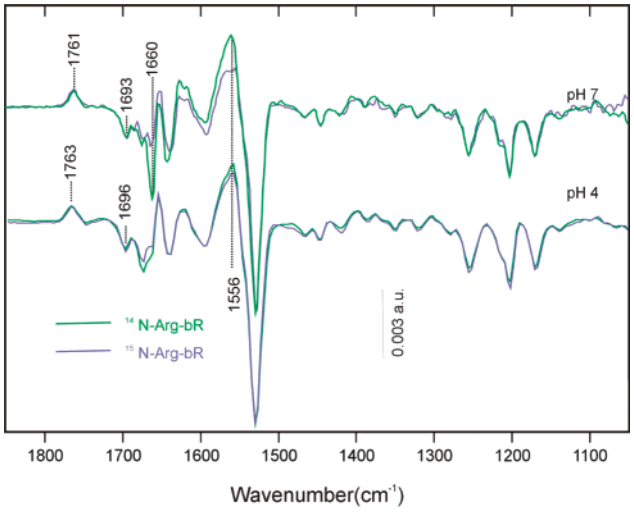

FIGURE 5: Average time-resolved FT-IR spectra of ^{14}N-Arg-bR (green) and ^{15}N-Arg-bR (purple) collected from 5 to 10 ms at 0 °C. The spectra have been scaled by the size of the negative band at 1527 cm^{-1}. The upper pair of traces was measured at pH 7 (and are taken from the same measurement as Figure 3a) and the lower pair at pH 4. Water contents in the pH 4 samples are within ~2% of each other for ^{14}N-Arg-bR and ^{15}N-Arg-bR and are ~65% (w/w). The pH is assumed not to have changed significantly from that of the buffer used to wash the sample, even though subsequent partial air-drying reduced the sample volume by a factor of 3−5.

show a C═O stretch of Asp-85 at 1761 cm^{-1} for pH 7 and at 1763 cm^{-1} for pH 4, i.e., a 2 cm^{-1} frequency difference that agrees with the previously reported value (*38*).

Our most important new observation at lower pH is the absence of the isotope-induced differences around 1556 and 1660 cm^{-1}, which are reproducibly observed at neutral pH conditions for two different samples. Instead, at the lower pH the isotopic variants show almost identical bR → M difference spectra. In both, the size of the positive 1556 cm^{-1} band (relative to other bands in the difference spectrum) is similar to that observed at higher pH only for the ^{15}N-Arg-bR sample. It is therefore concluded that the isotope-dependent shift of a positive M vibrational band at 1556 cm^{-1} can be observed only at higher pH, where fast H^+ release occurs.

Model Compound Studies. Figure 6 shows FT-IR spectra of the model compound *S*-decylthioethylguanidinium bromide (DTEG-Br) in chloroform equilibrated with an aqueous phase at various pH values. Protonated alkylguanidino groups generally absorb most strongly in the 1600−1700 cm^{-1} region. On the basis of prior model compound work (*46*), bands above 1600 cm^{-1} in Figure 6a are attributable to the two highest frequency C−N stretches of the ^{14}N-DTEG guanidino group, both of which have partial double bond character. These bands downshift 5−10 cm^{-1} in frequency for ^{15}N-DTEG, as shown in Figure 6b. However, as the pH is raised above ~11, there is a much larger frequency downshift of the C−N vibrational bands for both isotope variants of the DTEG model compound.

The most important observation is that, at the highest pH value (11.8), a distinct new band is clearly observed at 1554 cm^{-1} for ^{14}N-DTEG. In the ^{15}N-DTEG sample, this band downshifts and appears to split into two bands at 1541 and 1521 cm^{-1}. The pH dependence of the DTEG spectrum is consistent with the pK_a for the deprotonation being near 11,

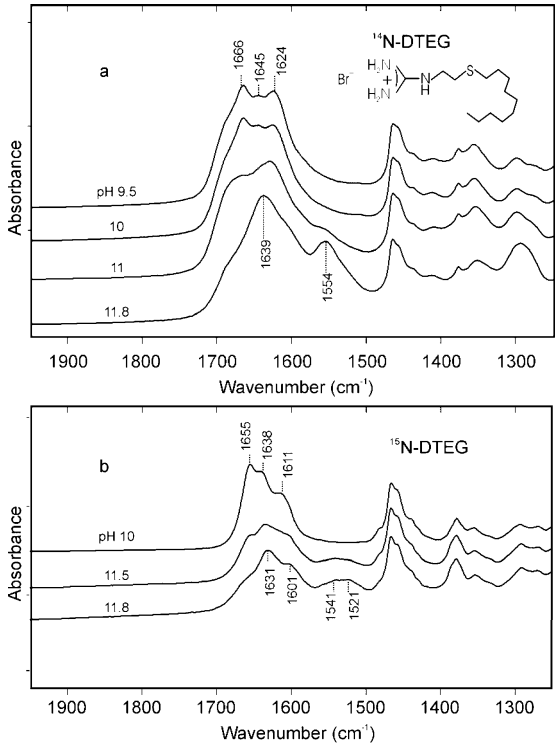

FIGURE 6: FT-IR spectra of DTEG with natural isotope abundance (upper panel) and with the two terminal nitrogens isotopically labeled with >90% ^{15}N (lower panel), measured in the chloroform phase previously equilibrated with an aqueous phase at the indicated pH values. Solvent backgrounds were subtracted, and then the spectra were normalized to the methylene vibrational band near 1460 cm^{-1}.

so that the 1554 cm^{-1} frequency for ^{14}N-DTEG corresponds to a deprotonated guanidine group. The most straightforward explanation for the frequency downshift of this band for ^{15}N-DTEG is that the band is due to a C−N stretch vibration of the guanidino group in its deprotonated form (*39*).

DISCUSSION

Our results are most consistent with the direct involvement of Arg-82 in the proton release group, undergoing at least partial deprotonation. This is in agreement with some previous proposals but not with alternatives that attribute fast proton release principally to (an)other amino acid side chain(s).

Primarily on the basis of their position within the bR three-dimensional structure, as well as on site-directed mutagenesis studies, previously proposed candidates for the PRG were Glu-204 and Glu-194 (*15*−*19*). However, the negative IR bands near 1700 cm^{-1} from these residues in the present bR → M difference spectrum are a factor of ~10 smaller than would be expected for a stoichiometric deprotonation, e.g., relative to the 1761 cm^{-1} positive band arising from protonation of Asp-85. This suggests that the observed Glu-204 and Glu-194 COOH difference bands are due to an H-bonding change, or at most a partial (~10%) deprotonation, as concluded previously by other FT-IR spectroscopists (*23*, *38*).

It has also been demonstrated that none of the bR → M vibrational difference bands attributable to COOH groups, including those assigned to Glu-194 and Glu-204, are significantly changed in intensity when the sample is

acidified to pH 4 (*38*). At this pH, early proton release is blocked because the pK_a of the PRG in the M state is 5.5−6. Thus, the observed COOH group IR difference bands seem to be unrelated to fast H^+ release.

Likewise, the amplitude and pH dependence of the submillisecond charge displacement associated with proton release, which has been detected by electrical measurements on bR, are inconsistent with proton transfer from the Schiff base to Asp-85 or with deprotonation of Glu-194 or Glu-204 to the bulk and, instead, clearly implicate a displacement of the Arg-82 side chain toward the extracellular surface (and/or its deprotonation) (*39*).

Nevertheless, on the basis of mutational studies it seems clear that Glu-194 and Glu-204 play some role in the fast H^+-release cascade, as exemplified by the delayed H^+ release in the E194Q (19) and E204Q mutants (*40*). Other workers have concluded that Glu-194 and/or Glu-204 contribute to an H-bonded network that helps to stabilize the deprotonated state of the PRG (*23*). The strongest evidence for this network is a broad continuum absorbance band, most easily observable from 1800 to 1900 cm^{-1}, caused by a structural rearrangement of the H-bonded network in the M state. All of the residues and water molecules that contribute to this network were proposed to help to stabilize the proton release group (*23*). Nevertheless, the changes in the H-bonded network upon M formation do not directly correspond to H^+ release, because the 1800−1900 cm^{-1} continuum absorbance shows the same time dependence at pH 7 and 5 (*23*), while fast H^+ release is observed only at the higher pH.

The location of Arg-82 within the folded bR structure (*8*, *41*), the known interaction of Arg-82 and Asp-85 (*42*, *43*), and the observation of a delay in H^+ release when Arg-82 is replaced with glutamine or alanine (*44*, *45*) have all made Arg-82 an important candidate for the PRG for nearly 15 years. Solid-state NMR experiments (*30*) have revealed that an arginine side chain, presumably Arg-82, gives anomalous ^{15}N resonances for the two terminal nitrogens in the M state at high pH. Furthermore, using site-directed mutagenesis combined with chemical/isotope labeling at Arg-82, Hutson et al. assigned a portion of the large positive band near 1550 cm^{-1} in the bR → M difference spectrum to Arg-82 in the M state (*21*). The absorbance change assignable to Arg-82 was comparable in size to the positive 1760 cm^{-1} band from Asp-85. However, neither the NMR nor the FT-IR paper cited above concluded that Arg-82 was the PRG. For the FT-IR experiment, assignment of 1550 cm^{-1} to a C−N stretch vibration of deprotonated Arg-82 in M was potentially in doubt because mutant proteins were used, and both R82A and R82C mutants have significantly different photocycle kinetics from those of wild-type bR at physiological pH (*21*).

Our reexamination of the role of Arg-82 in fast proton release with isotope-labeled wild-type bR is motivated by the previously reported 24 ppm splitting in the ^{15}N chemical shifts of the two terminal nitrogens of Arg-82 in the M state (*30*). Such a large perturbation should almost certainly affect the C−N stretch frequencies of Arg-82, resulting in large bR → M difference bands from Arg-82 in FT-IR spectra of wild-type bR. These C−N vibrational bands should naturally downshift when the terminal nitrogens of the guanidino group of arginines are labeled with a heavier isotope. Use of well-matched isotope variants guarantees that both proteins have identical photocycles, avoiding secondary effects that can cause difficulties in definitive band assignments.

Assignment of Bands at 1556 and 1660 cm^{-1} to Arg-82. At pH 7, where bR undergoes fast light-induced H^+ release, the bR → M difference spectrum of ^{14}N-Arg-bR reproducibly shows a larger positive 1556 cm^{-1} band than that of ^{15}N-Arg-bR (Figure 2). While L and M both show broad positive IR difference bands in the 1545−1560 cm^{-1} region, which have previously been associated with changes in amide II vibrations of the protein backbone, the band in this region that is sensitive to isotope labeling at arginine arises only when L decays to M. That is, in the bR → L difference spectra, no arginine-isotope-sensitive difference is observed (Figure 4a), whereas there is such arginine-isotope sensitivity in the bR → M difference spectra (Figure 4b). The downshifted frequency after ^{15}N substitution is near 1534 cm^{-1}, as shown in Figure 4b. This 22 cm^{-1} frequency downshift is consistent with the 24 cm^{-1} value expected for a pure C−N stretch vibration. Therefore, isotope labeling supports the assignment of a portion of the positive band at 1556 cm^{-1} to an arginine, presumably Arg-82, in the M state.

In addition, the bR → M difference spectrum of ^{14}N-Arg-bR also shows a negative band around 1660 cm^{-1} that loses intensity upon ^{15}N-labeling of the arginines (Figures 3 and 4b). Assignment of a 1660 cm^{-1} band to Arg-82 is consistent with the known frequencies of guanidino groups in model compounds, normally observed in the range of 1660−1675 cm^{-1} in polar environments (*46*). However, the only obvious candidate for a corresponding downshifted negative band in the ^{15}N-Arg-bR → M difference spectrum (Figure 3) is evidenced as a reduced positive doublet band near 1625 cm^{-1}, with which the downshifted negative band presumably overlaps. The isotope-shifted band is clearly visible as a distinct positive band centered at 1625 cm^{-1} in the double-difference spectrum (Figure 4b). The frequency difference from 1660 to 1625 cm^{-1} is somewhat greater than the 10−25 cm^{-1} downshifts typically calculated and observed for the highest frequency C−N stretch vibration of alkylguanidines upon ^{14}N → ^{15}N isotope substitution (*46*). However, this is attributable to the fact that protonated arginine has two strongly mixed intense C−N stretch vibrations in the 1610−1675 cm^{-1} range, and the overlapping bands complicate the observed intensity shifts (*46*). For example, the model compound examined in Figure 6, ^{14}N-DTEG dissolved in $CHCl_3$, shows a C−N stretch centered at 1666 cm^{-1} at pH values below 10, where the guanidino group is expected to be protonated. The band maximum downshifts to 1655 cm^{-1} upon ^{15}N substitution. But the isotope-induced IR absorption changes between 1620 and 1675 cm^{-1} are actually more complicated, with the largest ^{15}N-induced intensity decrease occurring above 1660 cm^{-1} and the most obvious intensity increase occurring near 1610 cm^{-1}. Taking into account the complexity of the isotope shift patterns in Figure 6, a large part of the negative 1660 cm^{-1} band in the bR → M difference spectrum can reasonably be attributed to a protonated arginine, presumably Arg-82, in the bR resting state changing structure upon M formation. The observed frequency of 1660 cm^{-1} for ^{14}N-Arg-bR supports the prior conclusion that Arg-82 in the bR state is in a typical hydrogen-bonded environment (*30*).

Assignment of a 1660 cm^{-1} band to Arg-82 takes into consideration the known frequencies of guanidino groups in

model compounds. Indeed, the model compound examined here, ^{14}N-DTEG dissolved in $CHCl_3$, shows a C−N stretch centered at 1666 cm^{-1} at pH values below 10, where the guanidino group is expected to be protonated. This frequency downshifts to 1655 cm^{-1} upon ^{15}N substitution. The ^{14}N → ^{15}N isotope substitution is expected to cause 5−10 cm^{-1} downshifts in the highest frequency C−N stretch vibration of alkylguanidines, normally observed in the range of 1660−1675 cm^{-1} in polar environments (*46*). This supports the prior conclusion that Arg-82 in the bR state is in a typical hydrogen-bonded environment (*30*).

On the other hand, 1556 cm^{-1} is well outside the expected ranges of C−N stretches of protonated alkylguanidino compounds (*46*). At the same time, our comparison of bR → M spectra from samples that differ only by ^{15}N substitution at terminal guanidine nitrogens of arginine residues provides very strong support for this C−N vibrational assignment in the M state. In addition, our ^{14}N-DTEG model compound shows an isotope-sensitive C−N stretch band at a similar frequency of 1556 cm^{-1} at pH 11.8, indicating that this is a characteristic frequency of alkylguanidino compounds under certain (unusual) conditions. The downshifted frequencies upon ^{15}N substitution in the region ∼1541−1521 cm^{-1} for the model compound and at 1534 cm^{-1} for the protein agree well with each other.

In a previous study of bR, a somewhat lower frequency than 1556 cm^{-1}, ∼1545 cm^{-1}, was reported for an unusual C−N stretch vibration of the guanidino group in the M state. However, this lower value was obtained only for "pseudo-Arg-82", i.e., from FT-IR difference spectra of samples of the R82C mutant with thioethylguanidinium attached via a disulfide linkage at the unique cysteine site (*21*). This structural difference is presumably responsible for the ∼11 cm^{-1} frequency difference between the two reported guanidino group C−N frequencies. The higher value (1556 cm^{-1}) more accurately reflects the C−N stretch frequency for Arg-82 in the M state of wild-type bR.

Our assignment of the 1556 cm^{-1} band in bR → M difference spectrum at pH 7 to an arginine vibration is based on its shift with ^{15}N-labeling of arginines. Confidence in this assignment depends on assurance that the frequency shift is not due to scrambling of the isotope to sites in the peptide backbone. However, scrambling by transamination would involve dilution of the ^{15}N into a much larger ^{14}N pool, resulting in a thin distribution of the diluted ^{15}N to numerous sites with uncoordinated behavior. In addition, when ^{14}C was used to trace the fate of the guanidino carbon in the arginine auxotroph (suitable radioisotopes of ^{15}N not being available), no detectable scrambling was found to other amino acid residues, lipid, or chromophore. Perhaps most decisive is the fact that the isotope-induced difference at 1556 cm^{-1} can be observed in bR → M difference spectra obtained at neutral pH but not at pH 4. This would be unexpected if there were a high level scrambling of ^{15}N over the peptide backbone, since amide II vibrational difference bands are also observed in the bR → M difference spectrum at the lower pH value. An identical bR → L difference spectrum for both proteins at pH 7 also indicates little scrambling. Therefore, we conclude that the frequency shift from 1556 to 1534 cm^{-1} upon ^{15}N substitution is due to highly specific labeling of arginines.

A further test for the assignment of a 1556 cm^{-1} band to Arg-82 is to compare the band's patterns for the M states of wild-type bR and Arg-82 mutants. The band is expected to disappear for mutants if our assignment is right. Comparison of time-resolved FT-IR difference spectra of wild-type bR and R82A shows that the latter indeed has a smaller positive band at this frequency (*21*). The intensity difference around this position can even be discerned from a visual comparison of 230 K static bR → M difference spectra of wild-type bR and the R82A, R82Q, and R82K mutants (*47*).

Deuteration Sensitivity. We did not repeat measurements of the bR → M difference spectrum in ^2H_2O, as these have been published before, and they support our assignment of a portion of the 1556 cm^{-1} band in the bR → M difference spectrum to Arg-82. In fact, this assignment helps to explain a previous puzzling question. It has been widely observed that, in the bR → M difference spectrum, some of the intensity at 1556 cm^{-1} appears to shift away when the spectrum is measured in ^2H_2O (*31*, *48*, *49*). Intensity shift at this position is so obvious that the 1568 cm^{-1} peak, due to the ethylenic stretch in M, could visibly be differentiated from the 1556 cm^{-1} band. Therefore, a portion of the band at 1556 cm^{-1} could be assigned to a group with a readily exchanged proton(s).

An obvious possibility is the backbone peptide. However, it has been concluded that the only "core" amide II modes, which exhibit exceedingly slow solvent H/D isotope exchange, contribute to the 1556 cm^{-1} band (*50*, *51*). In fact, an arginine, even one buried within the transport channel, would be more likely to undergo solvent exchange on the time scale of reported experiments and thereby give rise to the observed sensitivity of this band to ^2H_2O.

pH Dependence of the 1556 cm^{-1} Difference Band in M. Visual comparison of previously published bR → M difference spectra in the range between pH 4 and pH 9 clearly indicates a larger 1556 cm^{-1} band for pH values above ∼6, although this difference was not remarked upon by the previous workers (*23*, *38*). We have now reproduced this observation with great attention to performing adequate controls. The bR → M difference spectrum of ^{14}N-Arg-bR at pH 7 shows a larger 1556 cm^{-1} positive band than that at pH 4, as shown in Figure 6. When considering the fact that the fast H^+-release capability of bR decreases from pH ∼9.5 to pH ∼5, a significant implication of such dependence is that the relative intensity of the 1556 cm^{-1} band reflects the capacity of the bR to carry out fast light-induced H^+ release.

Identification of a group with a pH-dependent absorbance in the M state has been expected (*38*) but not previously accomplished. It is clear from Figure 5 that the pH-dependent portion of the absorbance at 1556 cm^{-1} in bR → M difference spectra is most likely from Arg-82. This conclusion is also consistent with the concept that core amide II vibrations contributing to the difference band at ∼1556 cm^{-1} (*50*) are as unlikely to show pH dependence as rapid H/D exchange.

In summary, a substantial portion of the 1556 cm^{-1} band in the bR → M difference spectrum, comparable in size to the 1760 cm^{-1} band due to the Asp-85 COOH group, is assignable to Arg-82, on the basis of all of the following characteristics: (i) it downshifts to ∼1534 cm^{-1} upon labeling of all seven arginines in bR with ^{15}N at the terminal nitrogens, (ii) it downshifts in $^{15}N_{\eta 2}$-labeled bR containing a "pseudoarginine" residue at position 82, inserted by a

combination of site-directed mutagenesis and chemical modification (*21*), (iii) it shows H/D exchangeability (*31*, *48*, *49*), and (iv) it disappears in Arg-82 mutants (*21*, *47*). If this assignment is correct, the question remains, under what conditions would the guanidine group exhibit a vibration at this unexpectedly low frequency?

Arginine-82 in M Is Most Likely at Least 50% Deprotonated. The assignment of a 1556 cm^{-1} band as arising in part due to an arginine vibrational frequency in the M state of wild-type bR is most simply explained if the guanidino group deprotonates. Only deprotonated guanidine compounds have ever been observed to show strong C−N stretch vibrations in the frequency range between 1500 and 1600 cm^{-1}. For example, spectra of ethylguanidine in 1 M sodium methoxide show that upon deprotonation some of the intensity associated with the most intense guanidine C−N stretch bands is downshifted to the region between 1500 and 1600 cm^{-1} (*46*). Our ^{14}N-DTEG model compound shows the C−N stretch vibration at ∼1556 cm^{-1}, with a further downshift to an apparent doublet at ∼1541 and ∼1521 cm^{-1} upon ^{15}N substitution at the two terminal nitrogens. Even in a nonpolar solvent such as $CHCl_3$, the frequencies below 1600 cm^{-1} only occur when the solvent is in equilibrium with aqueous solution at pH values above 11.8 (Figure 6), i.e., under conditions where the guanidino group is almost certainly deprotonated.

On the basis of the height of the double-difference band at 1556 cm^{-1} in Figure 4b, it is unlikely that it could arise from the participation of only a minor fraction of the arginine-82 in the sample. This band height is 1.8 ± 0.2 times as large as that of the 1761 cm^{-1} difference band that is widely accepted as representing a stoichiometric protonation of Asp-85 in M. While the extinction coefficient of a deprotonated guanidino group has not previously been published, it can be estimated from the known extinction coefficient of the protonated form and the titration spectra in Figure 6a. When all of the pH-dependent spectra are normalized to a band that is expected to be invariant with pH (specifically the CH_2 group vibration near 1450 cm^{-1}), the absorbance at 1660 cm^{-1} in the spectra at the two lowest pH values is 1 ± 0.5 times the absorbance at 1554 cm^{-1} (extrapolated from a fitted titration curve to limiting pH values). Therefore, the extinction coefficient at 1554 cm^{-1} for the deprotonated guanidine group is similar to the extinction coefficient at ∼1660 cm^{-1} for the protonated form. The peak values for protonated guanidino groups and protonated carboxylic acids in simple model compounds in aqueous solution were reported as 420 ± 40 and 280 ± 20 M^{-1} cm^{-1}, respectively (52), i.e., in a ratio of 1.5 ± 0.2. While the relative sizes of the guanidine group and carboxylic acid extinction coefficients might be affected significantly by environmental effects on bandwidths, it is unlikely that a ratio of <0.5 perturbed Arg-82 per protonated Asp-85 could give rise to the observed ratio (>1) of the 1556/1761 intensities associated with these groups in the M state IR difference spectrum. This conclusion is based on the assumption that the 1556 and 1761 cm^{-1} absorbance intensities measured from our samples are not significantly different from those expected for random orientation, a reasonable assumption given the samples' fairly high water content and the procedure for making them (i.e., squeezing concentrated pellets rather than drying onto the window).

The Nature of the Proton Release Group. Taken together, the foregoing would suggest that the rapidly released protons detected in the M state come mostly from Arg-82. In that case, the PRG should be identified as Arg-82. Such an identification is driven principally by FT-IR spectroscopy and may be controversial, given results from other techniques.

First, although the 24 ppm splitting of the ^{15}N chemical shift values of the η-nitrogens of Arg-82 in the M state (*30*) is very large compared to those of protonated arginines, it is still significantly smaller than the 42 ppm measured for deprotonated arginine in an aqueous medium (*53*). Furthermore, the average of the chemical shifts of the two η-nitrogens of Arg-82 in the M state is somewhat further upfield than has been observed for deprotonated guanidinyl compounds in aqueous solutions (*54*).

The measured pK_a of the PRG in the M state, 5.8 (*14*), is also quite low to be associated with an arginine. However, in the bR → M transition there is a widely agreed >8 unit pK_a increase for Asp-85. Its pK_a is ∼2.5 in the resting state (*42*) but rises to be >11 in the long-lived M intermediate (*55*). This >8 unit increase in pK_a for Asp-85 has been attributed to a large transient decrease in its local dielectric constant, which would destabilize the deprotonated (ionized) form in the M state (*55*). A similar effect would be expected instead to lower the pK_a of Arg-82, for which the destabilized charged form is the protonated species. Significant changes in the environment around Arg-82 have indeed been observed in an atomic resolution X-ray structure of the M state (*56*). In particular, the side chain of Arg-82 moves substantially closer to the extracellular surface, and this shifted position leads to a reduction in the number of hydrogen bonds to its guanidino group.

Finally, while fast H^+ release is abolished in the R82Q mutant of bR below pH 7.5, it is restored above pH 7.5 (*57*). Similarly, it is observed in R82Q/D212N over a wide pH range (*58*). These results from arginine mutants indicate that deprotonation of Arg-82 is not required for H^+ release in M. In fact, however, the presence of fast H^+ release in Arg-82 mutants under limited conditions argues only superficially against the role of Arg-82 in the release. Even if the released H^+ in wild-type bR comes predominantly from Arg-82, it could be involved in a rapid equilibrium among various sites within a hydrogen-bonded complex. It is expected that a different H^+ equilibrium would exist among these sites for Arg-82 mutants. What this means is that although Arg-82 would function as the source of the fast released H^+ in wild-type bR, in Arg-82 mutants another residue, or water, could become the source of the fast released H^+. This would not be the first protein in which built-in redundancy allows function to be maintained even after the elimination of a residue that normally carries out that function. One must therefore be very careful in drawing a conclusion about the functioning of the wild-type protein from the retention of activity in mutants.

Our identification of Arg-82 as the proton release group (PRG) depends on using the original literature definition of this phrase (*44*). With this definition, the PRG is understood to signify the source in the bR state of protons released to the extracellular medium before Asp-85 is restored to its deprotonated state at the end of the photocycle. By this definition the PRG must be protonated in the unphotolyzed

bR state and deprotonated in the M state at pH 7 but not deprotonated in the M state formed at pH 4. Other than the retinylidene Schiff base itself, which transfers its proton to Asp-85 (*8*), the only group for which there is any direct spectroscopic evidence for a roughly stoichiometric deprotonation between bR and M at pH 7 is Arg-82 (as discussed above); this spectroscopic signature is furthermore absent at pH 4.

However, crystal structures show clearly that Arg-82 is not in H-bonding contact with bulk water in either the bR or M state (*7*), and therefore the H^+ release pathway to the extracellular medium must involve intermediate transfers to and from other groups, e.g., Glu-194 or Glu-204 or other components of an H-bonded network (*19*, *20*, *23*), within what has been called the proton release complex, PRC (*20*). Thus Arg-82 is probably not the "terminal proton transfer group", which we would define as the last group within the PRC to carry the proton transiently prior to its transfer to an H_2O molecule in the bulk extracellular medium. This function is still quite reasonably attributed to Glu-194 or Glu-204 (*16*, *19*) even though the most thorough FT-IR investigations indicate that they are likely protonated to a similar degree in both bR and M (*23*, *38*).

Modeling the Causes of the Arginine Deprotonation. We offer the following hypotheses to account for the proposed protonation change at Arg-82 during the L → M transition. The mutual stabilization between negatively charged Asp-85 and positively charged Arg-82 in the bR resting state disappears in M, due largely to the protonation of Asp-85 and possibly also to the loss of water molecules in this region of the protein. These environmental changes around Arg-82 cause its positively charged guanidino group to be situated in a much less favorable dielectric environment. This could largely account for its lowered pK_a in the M state.

Although the fast released H^+ is at least partially from Arg-82, the "proton deficit" in the M state is likely to be spread among various sites through H-bonding directly with water and indirectly with other components of a hydrogen-bonded complex, including Tyr-83, Glu-194, Glu-204, and additional H_2O molecules. The transfer of the proton from the arginine to the surface is likely to occur at a rate that strongly depends on the structure of the entire web of H-bonding partners, which could explain why all of them affect the kinetics of fast H^+ release (*16*, *19*, *20*, *23*).

REFERENCES

1. Herzfeld, J., and Lansing, J. C. (2002) Magnetic resonance studies of the bacteriorhodopsin pump cycle, *Annu. Rev. Biophys. Biomol. Struct. 31*, 73−95.
2. Neutze, R., Pebay-Peyroula, E., Edman, K., Royant, A., Navarro, J., and Landau E. M. (2002) Bacteriorhodopsin: a high-resolution structural view of vectorial proton transport, *Biochim. Biophys. Acta 1565*, 144−167.
3. Lanyi, J. K. (2004) Bacteriorhodopsin, *Annu. Rev. Physiol. 66*, 665−688.
4. Mathies, R. A., Lin, S. W., Ames, J. B., and Pollard, W. T. (1991) From femtoseconds to biology: Mechanism of bacteriorhodopsin's light-driven proton pump, *Annu. Rev. Biophys. Biophys. Chem. 20*, 491−518.
5. Mathies, R. A., Brito, C. C. H., Pollard, W. T., and Shank, C. V. (1988) Direct observation of the femtosecond excited-state cis−trans isomerization in bacteriorhodopsin, *Science 240*, 777−779.
6. Dobler, J., Zinth, W., Kaiser, W., and Oesterhelt, D. (1988) Excited-state reaction dynamics of bacteriorhodopsin studied by femtosecond spectroscopy, *Chem. Phys. Lett. 144*, 215−220.
7. Sass, H. J., Buldt, G., Gessenich, R., Hehn, D., Neff, D., Schlesinger, R., Berendzen, J., and Ormos, P. (2000) Structural alterations for proton translocation in the M state of wild-type bacteriorhodopsin, *Nature 406*, 649−653.
8. Braiman, M. S., Mogi, T., Marti, T., Stern, L. J., Khorana, H. G., and Rothschild, K. J. (1988) Vibrational spectroscopy of bacteriorhodopsin mutants: Light-driven proton transport involves protonation changes of aspartic acid residues 85, 96, and 212, *Biochemistry 27*, 8516−8520.
9. Xie A. H., Nagle J. F., and Lozier R. H. (1987) Flash spectroscopy of purple membrane, *Biophys. J. 51*, 627−635.
10. Heberle, J., and Dencher, N. A. (1992) Surface-bound optical probes monitor proton translocation and surface potential changes during the bacteriorhodopsin photocycle, *Proc. Natl. Acad. Sci. U.S.A. 89*, 5996−6000.
11. Alexiev, U., Mollaaghababa, R., Scherrer, P., Khorana, H. G., and Heyn, M. P. (1995) Rapid long-range proton diffusion along the surface of the purple membrane and delayed proton transfer into the bulk, *Proc. Natl. Acad. Sci. U.S.A. 92*, 372−376.
12. Cao, Y., Brown, L. S., Sasaki, J., Maeda, A., Needleman, R., and Lanyi, J. K. (1995) Relationship of proton release at the extracellular surface to deprotonation of the schiff base in the bacteriorhodopsin photocycle, *Biophys. J. 68*, 1518−1530.
13. Siebert, F., Mäntele, W., and Kreutz, W. (1982) Evidence for the protonation of two internal carboxylic groups during the photocycle of bacteriorhodopsin: Investigation of kinetic infrared spectroscopy, *FEBS Lett. 141*, 82−87.
14. Zimányi, L., Váró, G., Chang, M., Ni, B., Needleman, R., and Lanyi, J. K. (1992) Pathways of proton release in the bacteriorhodopsin photocycle, *Biochemistry 31*, 8535−8543.
15. Brown, L. S., Needleman, R., and Lanyi, J. K. (1996) Interaction of proton and chloride transfer pathways in recombinant bacteriorhodopsin with chloride transport activity: Implications for the chloride translocation mechanism, *Biochemistry 35*, 16048−16054.
16. Brown, L. S., Sasaki, J., Kandori, H., Maeda, A., Needleman, A., and Lanyi, J. K. (1995) Glutamic acid 204 is the terminal proton release group at the extracellular surface of bacteriorhodopsin, *J. Biol. Chem. 270*, 27122−27126.
17. Richter, H. T., Brown, L. S., Needleman, R., and Lanyi, J. K. (1996) A linkage of the pK_a's of asp-85 and glu-204 forms part of the reprotonation switch of bacteriorhodopsin, *Biochemistry 35*, 4054−4062.
18. Richter, H. T., Needleman, R., Kandori, H., Maeda, A., and Lanyi, J. K. (1996) Relationship of retinal configuration and internal proton transfer at the end of the bacteriorhodopsin photocycle, *Biochemistry 35*, 15461−15466.
19. Dioumaev, A. K., Richter, H. T., Brown, L. S., Tanio, M., Satoru, T., Saito, H., Kimura, Y., Needleman, R., and Lanyi, J. K. (1998) Existence of a proton transfer chain in bacteriorhodopsin: Participation of glu-194 in the release of protons to the extracellular surface, *Biochemistry 37*, 2496−2506.
20. Balashov, S. P., Govindjee R., Imasheva, E. S., Misra, S., Ebrey, T. G., Feng, Y., Crouch, P. K., and Menick, D. R. (1995) The two pK_a's of aspartate-85 and control of thermal isomerization and proton release in the arginine-82 to lysine mutant of bacteriorhodopsin, *Biochemistry 34*, 8820−8834.
21. Hutson, M. S., Alexiev, U., Shilov, S. V., Wise, K. J., and Braiman, M. S. (2000) Evidence for a perturbation of arginine-82 in the bacteriorhodopsin photocycle from time-resolved infrared spectra, *Biochemistry 39*, 13189−13200.
22. Kono, M., Misra, S., and Ebrey, T. G. (1993) pH dependence of light-induced proton release by bacteriorhodopsin, *FEBS Lett. 331*, 31−34.
23. Rammelsberg, R., Huhn, G., Lübben, M., and Gerwert, K. (1998) Bacteriorhodopsin's intramolecular proton-release pathway consists of a hydrogen-bonded network, *Biochemistry 37*, 5001−5009.
24. Spassov, V. Z., Luecke, H., Gerwert, K., and Bashford, D. (2001) pK_a calculations suggest storage of an excess proton in a hydrogen-bonded water network in bacteriorhodopsin, *J. Mol. Biol. 312*, 203−219.
25. Braiman, M. S., Bousché, O., and Rothschild, K. J. (1991) Protein dynamics in the bacteriorhodopsin photocycle: Submillisecond Fourier transform infrared spectra of the L, M, and N photointermediates, *Proc. Natl. Acad. Sci. U.S.A. 88*, 2388−2392.
26. Bousché, O., Sonar, S., Krebs, M. P., Khorana, H. G., and Rothschild, K. J. (1992) Time-resolved Fourier transform infrared spectroscopy of the bacteriorhodopsin mutant tyr-185→phe: asp-96 reprotonates during O formation; asp-85 and asp-212 deprotonate during O decay, *Photochem. Photobiol. 56*, 1085−1095.

27. Gerwert, K., Souvignier, G., and Hess, B. (1990) Simultaneous monitoring of light-induced changes in protein side-group protonation, chromophore isomerization, and backbone motion of bacteriorhodopsin by time-resolved Fourier-transform infrared spectroscopy, *Proc. Natl. Acad. Sci. U.S.A. 87*, 9774−9778.
28. Dencher, N. A., and Wilms, M. (1975) Flash photometric experiments on the photochemical cycle of bacteriorhodopsin, *Biophys. Struct. Mech. 1*, 259−271.
29. Cao Y., Brown, L. S., Needleman, R., and Layni, J. K. (1993) Relationship of proton uptake on the cytoplasmic surface and reisomerization of the retinal in the bacteriorhodopsin photocycle: An attempt to understand the complex kinetics of the pH changes and the N and O intermediates, *Biochemistry 32*, 10239−10248.
30. Petkova, A. T., Hu, J. G., Bizounok, M., Simpson, M., Griffin, R. G., and Herzfeld, J. (1999) Arginine activity in the protonmotive photocycle of bacteriorhodopsin: Solid-state NMR studies of the wild-type and D85N proteins, *Biochemistry 38*, 1562−1572.
31. Braiman, M. S., Ahl, P. L., and Rothschild, K. J. (1987) Millisecond Fourier-transform infrared difference spectra of bacteriorhodopsin's M412 photoproduct, *Proc. Natl. Acad. Sci. U.S.A. 84*, 5221−5225.
32. Doherty, D. G., Shapira, R. H., and Burnett, W. T. (1957) Synthesis of aminoalkylisothiuronium salts and their conversion to mercaptoalkylguanidines and thiazolines, *J. Am. Chem. Soc. 79*, 5667−5671.
33. Chizhov, I., Chernavskii, D. S., Engelhard, M., Mueller, K. H., Zubov, B. V., and Hess, H. (1996) Spectrally silent transitions in the bacteriorhodopsin photocycle, *Biophys. J. 71*, 2329−2345.
34. Rödig, C., Chizhov, I., Weidlich, O., and Siebert, F. (1999) Time-resolved step-scan Fourier transform infrared spectroscopy reveals differences between early and late M intermediates of bacteriorhodopsin, *Biophys. J. 76*, 2687−2701.
35. Sharonov, A. Yu., Tkachenko, N. V., Savransky, V. V., and Dioumaev, A. K. (1991) Time-resolved ultraviolet absorption changes in the photocycle of bacteriorhodopsin, *Photochem. Photobiol. 54*, 889−893.
36. Dioumaev, A. K. (1997) Evaluation of intrinsic chemical kinetics and transient product spectra from time-resolved spectroscopic data, *Biophys. Chem. 67*, 1−25.
37. Sasaki, J., Lanyi, J. K., Needleman, R., Yoshizawa, T., and Maeda, A. (1994) Complete identification of CO stretching vibrational bands of protonated aspartic acid residues in the difference infrared spectra of M and N intermediates versus bacteriorhodopsin, *Biochemistry 33*, 3178−3184.
38. Zscherp, C., Schlesinger, R., Tittor, J., Oesterhelt, D., and Heberle. J. (1999) In situ determination of transient pK_a changes of internal amino acids of bacteriorhodopsin by using time-resolved attenuated total reflection Fourier-transform infrared spectroscopy, *Proc. Natl. Acad. Sci. U.S.A. 96*, 5498−5503.
39. Dickopf, S., and Heyn, M. P. (1997) Evidence for the first phase of the reprotonation switch of bacteriorhodopsin from time-resolved photovoltage and flash photolysis experiments on the photoreversal of the M-intermediate, *Biophys J. 73*, 3171−3181.
40. Misra, S., Govindjee, R., Ebrey, T. G., Chen, N., Ma, J. X., and Crouch, R. K. (1997) Proton uptake and release are rate-limiting steps in the photocycle of the bacteriorhodopsin mutant E204Q, *Biochemistry 36*, 4875−4883.
41. Henderson, R., Baldwin, J. M., Ceska, T. A., Zemlin, F., Beckmann, E., and Downing, K. H. (1990) Model for the structure of bacteriorhodopsin based on high-resolution electron cryomicroscopy, *J. Mol. Biol. 213*, 899−929.
42. Subramaniam, S., Marti, T., and Khorana, H. G. (1990) Protonation state of asp (glu)-85 regulates the purple-to-blue transition in bacteriorhodopsin mutants arg-82- - -ala and asp-85- - -glu: the blue form is inactive in proton translocation, *Proc. Natl. Acad. Sci. U.S.A. 87*, 1013−1017.
43. Thorgeirsson, T. E., Milder, S. J., Miercke, L. J., Betlach, M. C., Shand, R. F., Stroud, R. M., and Kliger, D. S. (1991) Effects of asp-96→asn, asp-85→asn, and arg-82→gln single-site substitutions on the photocycle of bacteriorhodopsin, *Biochemistry 30*, 9133−9142.
44. Brown, L. S., Bonet, L., Needleman, R., and Lanyi, J. K. (1993) Estimated acid dissociation constants of the Schiff base, asp-85, and arg-82 during the bacteriorhodopsin photocycle, *Biophys. J. 65*, 124−130.
45. Otto, H., Marti, T., Holz, M., Mogi, T., Stern, L. J., Engel, F., Khorana, H. G., and Heyn, M. P. (1990) Substitution of amino acids asp-85, asp-212, and arg-82 in bacteriorhodopsin affects the proton release phase of the pump and the p*K* of the Schiff base, *Proc. Natl. Acad. Sci. U.S.A. 87*, 1018−1022.
46. Braiman, M. S., Briercheck, D. M., and Kriger, K. M. (1999) Modeling vibrational spectra of amino acid side chains in proteins: effects of protonation state, counterion, and solvent on arginine C−N stretch frequencies, *J. Phys. Chem. B 103*, 4744−4750
47. Hatanaka, M., Sasaki, J., Kandori, H., Ebrey, T. G., Needleman, R., Lanyi, J. K., and Maeda, A. (1996) Effects of arginine-82 on the interactions of internal water molecules in bacteriorhodopsin, *Biochemistry 35*, 6308−6312.
48. Bagley, K., Dollinger, G., Eisenstein, L., Singh, A. K., and Zimányi, L. (1982) Fourier transform infrared difference spectroscopy of bacteriorhodopsin and its photoproducts, *Proc. Natl. Acad. Sci. U.S.A. 79*, 4972−4976.
49. Grieger, I., and Atkinson, G. H. (1985) Photolytic interruptions of the bacteriorhodopsin photocycle examined by time-resolved resonance Raman spectroscopy, *Biochemistry 24*, 5660−5665.
50. Kluge, T., Olejnik, J., Smilowitz, L., and Rothschild, K. J. (1998) Conformational changes in the core structure of bacteriorhodopsin, *Biochemistry 37*, 10279−10285.
51. Rothschild, K. J., Marti, T., Sonar, S., He, Y., Rath, P., Fischer, W., and Khorana, H. G. (1993) Asp96 deprotonation and transmembrane alpha-helical structural changes in bacteriorhodopsin, *J. Biol. Chem. 268*, 27046−27052.
52. Venyaminov, S., and Kalnin, N. N. (1990) Quantitative IR spectrophotometry of peptide compounds in water (H_2O) solution. I. Spectral parameters of amino acid residue absorption bands, *Biopolymers 30*, 1243−1257.
53. Kanamori, K., and Roberts, J. D. (1983) A nitrogen-15 NMR study of the barriers to isomerization about guanidinium and guanidino carbon−nitrogen bonds in L-arginine, *J. Am. Chem. Soc. 105*, 4698−4701.
54. Levy, G. C., and Lichter, R. L. (1979) *Nitrogen-15 Nuclear Magnetic Resonance Spectroscopy*, Wiley-Interscience, New York.
55. Braiman, M. S., Dioumaev, A. K., and Lewis, J. R. (1996) A large photolysis-induced pK_a increase of the chromophore counterion in bacteriorhodopsin: implications for ion transport mechanisms of retinal proteins, *Biophys. J. 70*, 939−947.
56. Luecke, H., Schobert, B., Richter, H., Cartailler, J., and Lanyi, J. K. (1999) Structural changes in bacteriorhodopsin during ion transport at 2 angstrom resolution, *Science 286*, 255−260.
57. Govindjée, R., Misra, S., Balashov, S. P., Ebrey, T. G., Crouch, R. K., and Menick, D. R. (1996) Arginine-82 regulates the pK_a of the group responsible for the light-driven proton release in bacteriorhodopsin, *Biophys. J. 71*, 1011−1023.
58. Brown, L. S., Váró, G., Hatanaka, M., Sasaki, J., Kandori, H., Maeda, A., Friedman, N., Sheves, M., Needleman, R., and Lanyi, J. K. (1995) The complex extracellular domain regulates the deprotonation and reprotonation of the retinal Schiff base during the bacteriorhodopsin photocycle, *Biochemistry 34*, 12903−12911.

BI049238G